Biodistribution, Dosimetry, and Clinical Evaluation of Technetium-99m Ethyl Cysteinate Dimer in Normal Subjects and in Patients with Chronic Cerebral Infarction

B. Leonard Holman, Robert S. Hellman, Stanley J. Goldsmith, Ismael G. Mena, Jean Leveille, Paolo Gerundini Gherardi, Jean-Luc Moretti, Angelika Bischof-Delaloye, Thomas C. Hill, Pierre M. Rigo, Ronald L. Van Heertum, Peter J. Ell, Udalrich Buell, Michel C. De Roo, and Robert A. Morgan

Department of Radiology, Brigham and Women's Hospital and Harvard Medical School, Boston, Massachusetts; Medical College of Wisconsin, Milwaukee, Wisconsin; Mt. Sinai Medical Center, New York, New York; Harbor-UCLA Medical Center, Torrance, California; Hotel Dieu de Montreal, Montreal, Canada; Istituto Scientifico,, S. Raffaele, Milano, Italy; Hospital Avicenne, Bobigny, France; Centre Hospitalier Universitaire Vaudois, School of Medicine, Lausanne, Switzerland; New England Deaconess Hospital, Boston, Massachusetts; Hopital de Baviere, Liege, Belgium; St. Vincents Hospital, New York, New York; University College and Middlesex School of Medicine, London, England; Abteilung Nulkearmedizin, Technical University of Aachen, West Germany; Universitaire Ziekenhuizen, Gasthuisberg, Leuven, Belgium; and Dupont Company, North Billerica, Massachusetts

Technetium-99m ethyl cysteinate dimer (ECD) has high initial cerebral uptake with slow clearance in nonhuman primates suggesting ideal characteristics for single photon emission computer tomography (SPECT) imaging. We evaluated the biodistribution, dosimetry and scintigraphic pattern of [^{99m}Tc]ECD in normal subjects and the accuracy of SPECT imaging in patients with chronic cerebral infarction. Sixteen normal subjects were injected with ~10 mCi of [^{99m}Tc]ECD. Anterior and posterior single-pass whole-body images were obtained at multiple times after injection. Blood clearance of the radiotracer was rapid, falling to 10.0 ± 6.6% and 4.9 ± 1.1% of the injected dose at 2 and 60 min, respectively. Brain uptake was 6.4 ± 2.1% of the injected dose 5 min after injection. The critical organ was the urinary bladder. Technetium-99m ECD SPECT was performed with a rotating gamma camera in ten of the 16 normal subjects and 34 patients with clinical and CT evidence of chronic stroke. Thirty-three of the thirty-four patients had focal [^{99m}Tc]ECD abnormalities on SPECT (97.1%) based on visual inspection of the SPECT images. In summary, we obtained high quality SPECT images as a result of the optimal physical and biologic characteristics of the tracer. Technetium-99m ECD SPECT shows promise for the evaluation of patients with stroke.

J Nucl Med 30:1018–1024, 1989

The introduction of single photon emission computed tomography (SPECT) perfusion imaging of the brain required the development of radiotracers that are lipophilic and that move across the blood-brain barrier efficiently, so that uptake is proportionate to cerebral blood flow. For these tracers to be useful with imaging devices such as the rotating gamma camera, their rate of clearance from the brain must be relatively slow and their intracerebral distribution should be fixed during the 20–30 min required for imaging.

Iodine-123 isopropyl iodoamphetamine ([^{123}I]IMP) was the first of these radiotracers to be applied successfully to SPECT imaging of the human brain (*1,2*). Iodine-123 IMP crosses the blood-brain barrier rapidly with ~6–7% of the injected dose remaining in the brain

Received Oct. 24, 1988; revision accepted Feb. 7, 1988.

For reprints contact: B. Leonard Holman, MD, Dept. of Radiology, Brigham and Women's Hospital, 75 Francis St., Boston, MA 02115.

20 min after intravenous injection. While the tracer redistributes significantly by 3–4 hr, the activity is sufficiently fixed for satisfactory rotating gamma camera SPECT within the first hour after injection (*3*). This methodology has been useful in the evaluation of a wide range of cerebrovascular and neurologic diseases including stroke (*4,5*), dementia (*6*), and epilepsy (*7*).

The less than optimal physical characteristics of ^{123}I including high-energy contamination and a relatively high patient radiation dose and the failure to develop an efficient commercial distribution system for [^{123}I] IMP stimulated a search for a technetium-99m- (^{99m}Tc) based brain perfusion agent. Technetium-99m PnAO and its analog, [^{99m}Tc]HM-PAO, were the first successfully applied ^{99m}Tc radiotracers (*8,9*). Another class of compounds was based on the diamine dithiol (DADT) backbone. Exploration of this class of ^{99m}Tc compounds led to the identification of several members with high initial cerebral extraction but with rapid clearance (*10,11*). Recently, a more promising member of this class, ^{99m}Tc ethyl cysteinate dimer (ECD), has been synthesized (*12*). Technetium-99m ECD displayed high initial cerebral uptake and slow clearance in nonhuman primates, suggesting ideal characteristics for SPECT imaging (*13*). We therefore determined the biodistribution, dosimetry, and scintigraphic pattern of [^{99m}Tc] ECD in normal subjects and the accuracy of [^{99m}Tc] ECD SPECT imaging in patients with documented chronic cerebral infarction.

METHODS

Preparation of the Radiopharmaceutical

Technetium-99m ECD (ethyl cysteinate dimer, DuPont Company No. Billerica, MA) was prepared from two vials, one containing a sterile and nonpyrogenic lyophilized mixture and the other a liquid phosphate buffer. Saline (1.2 ml) was injected into the first vial to dissolve its contents. The contents of the first vial then were transferred into the second and 25 mCi (0.5 ml) of ^{99m}Tc generator eluant was injected into the second vial. The mixture was allowed to stand at room temperature for 15 min. The radiochemical purity of the final solution was determined by thin layer chromatography.

Biodistribution

The biodistribution study was carried out at four laboratories (Brigham and Women's Hospital, Medical College of Wisconsin, Mt. Sinai Medical Center, and Harbor-UCLA Medical Center). Sixteen normal subjects (13 males, three females) were injected with ~10 mCi of [^{99m}Tc]ECD. All volunteers fasted for 4 hr prior to injection of [^{99m}Tc]ECD and none were on medication. All were in good physical health with no history of central nervous system or cerebrovascular disease.

Anterior and posterior single pass whole-body images were obtained using a state-of-the-art Anger scintillation camera starting at 5 min postinjection with a scan speed of 20 cm/min. Imaging was repeated at 30, 60, and 120 min and at 4, 24, and 48 hr postinjection. Regions of interest (ROIs) encompassing the entire organ in both the anterior and posterior views were obtained at each time point for brain, thyroid, lung, heart, liver, spleen, gallbladder, kidney, bladder, and legs. The ROI for the colon was determined at 4, 24, and 48 hr. In addition, venous blood samples were obtained at 0.5, 1, 2, 3, 4, 5, 10, 15, 30, 60, and 240 min and 24 hr after injection; urine was collected at 2, 4, 6, and 24 hr; and feces was collected up to 48 hr.

The geometric mean net count was determined for each organ for each time point by obtaining the square root of the product of the net anterior counts and the net posterior counts at that time point. The injected dose was determined as the square root of the product of the 5-min anterior whole-body net count and the 5-min posterior whole-body net count after correction for physical decay. The percent injected dose for each organ was determined at each time point.

The percent total injected dose present in the blood and in urine and feces was determined at various times postinjection. The percent injected dose of the radiotracer present in the blood was determined using standard predicted normal blood volume values for men and for women.

Radiation dose estimates were calculated at Oak Ridge Associated Universities from the biodistribution data using their MIRDose computer program.

SPECT Protocol

SPECT was performed in ten normal subjects (eight males, two females) and 34 patient volunteers (26 males, eight females). Each patient had been diagnosed as having a stroke more than 4 wk prior to the study based on clinical neurologic signs and symptoms and the subsequent development of an abnormal computed tomography (CT) scan. A reference current (within 48 hr of the study) CT scan was obtained with the reference plane oriented so that the orbitomeatal line was parallel to the plane of the gantry.

Technetium-99m ECD (10–30 mCi) was injected intravenously. Between 20 min and 2 hr after administration of the radiotracer, SPECT imaging was performed using a state-of-the-art rotating gamma camera with in-plane spatial resolution of 18 mm full width at half maximum or better. Images were acquired in a 64 × 64 image matrix over a 360-degree rotation in three degree increments. A minimum of 60,000 counts per view were obtained with an upper limit of 20 sec of acquisition per view.

Tomographic data were reconstructed using a nine-point weighted spatial or two-dimensional FFT prereconstruction filter to remove image noise. A ramp filter was applied during image reconstruction without postreconstruction image filtering. Reconstructed images were corrected for uniformity, attenuation, and deviation from the center of rotation. A linear attenuation coefficient of 0.12 cm^{-1} was applied. Images were reconstructed in the transverse, sagittal, and coronal planes. Each slice thickness was 1 pixel or 0.625 cm.

From the transaxial data set, a line along the interhemispheric fissure was divided into four equal segments. Lines were drawn perpendicular to the interhemispheric fissure at the intersections of the segments, dividing each hemisphere into four rectangular regions of interest (Fig. 1). The [^{99m}Tc] ECD SPECT studies in the 34 patients with stroke and ten normal patients were interpreted by one physician (BLH) blinded to the clinical laboratory data including the results of

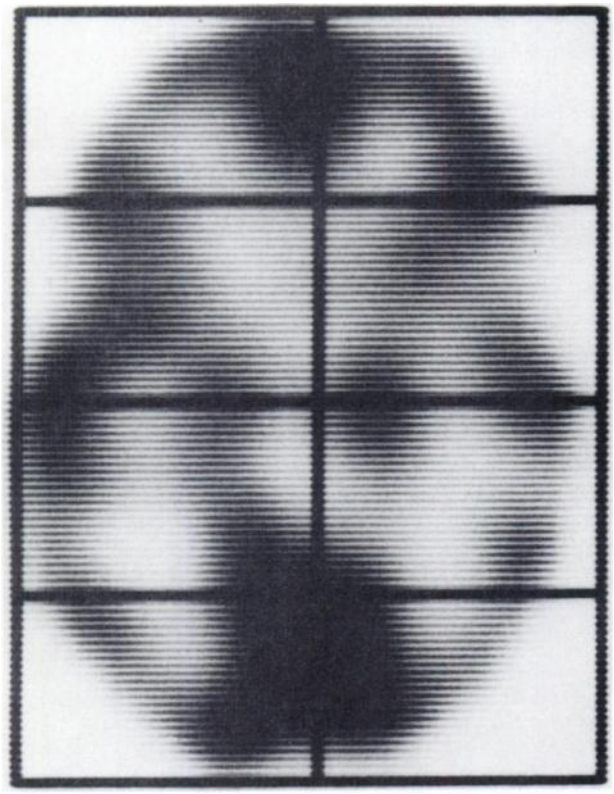

FIGURE 1
Matrix used to divide each hemisphere into four ROIs.

the CT examination. The interpretations were compared to the nonblinded interpretation of the principle investigator from the laboratory of origin. Discrepancies were noted and the blinded interpretation was used for final data analysis.

The images were also visually assessed to detect the presence of decreased tracer uptake in each of the regions. The transaxial CT images were likewise divided into four regions per hemisphere. The presence of focal areas of decreased tissue density, representing tissue necrosis or edema, was localized within the corresponding regions in each of the patients.

RESULTS

Biodistribution and Dosimetry

Blood clearance of the radiotracer was rapid, falling to 10.0 ± 6.6% of the injected dose at 2 min, 7.4 ± 3.0% ID at 30 min and 4.9 ± 1.1% of the injected dose at 60 min after injection (Fig. 2). Clearance of the tracer was primarily through the kidneys with 49.4 ± 13.5% of the injected dose in the urine by 2 hr and 71.5 ± 10.1% by 24 hr after injection. Only 11.5 ± 4.8% of the injected dose was excreted through the hepatobiliary system by 48 hr after injection.

Brain uptake was 6.4 ± 2.1% of the injected dose 5 min after injection falling slowly to 3.7 ± 0.3% 4 hr after injection (Table 1). The loss of brain activity from the planar whole-body images (without background subtraction) was 10.4% (20.8%/hr) from 5–30 min, 9.8% (19.6%/hr) from 30–60 min, 8.1% (8.1%/hr) from 1–2 hr and 20.3% (10.1%/hr) from 2–4 hr after injection. Gallbladder activity peaked at 4.2 ± 3.2% of the injected dose 2 hr after the injection falling to 1.8 ± 1.5% ID at 4 hr. Liver activity fell from 15.0 ± 8.9% of the injected dose at 5 min after injection to 9.0 ± 6.2% ID at 30 min and 5.4 ± 4.1% ID at 60 min. Lung clearance was rapid with only 4.6 ± 3.0% of the injected dose in the lungs 5 min after injection.

The critical organ is the urinary bladder wall with an estimated radiation dose of 0.27 rad/mCi assuming a 4.8-hr void or 0.11 rad/mCi assuming a 2.0-hr void. The dose to other organs was substantially lower with the large intestinal wall receiving ~0.05 rad/mCi and the gallbladder wall 0.09 rad/mCi (Table 2).

SPECT

In the 34 patients with chronic stroke, a single stroke of 1 mo or greater duration was present on CT in 31 and multiple strokes were present in three patients (three in one patient and two in two patients). Of the 38 strokes in the 34 patients, 18 involve the right hemisphere while 20 involve the left.

The technical quality of the SPECT images was high in all 34 patients and ten normal volunteers. There was excellent delineation of the cortical gray matter, basal

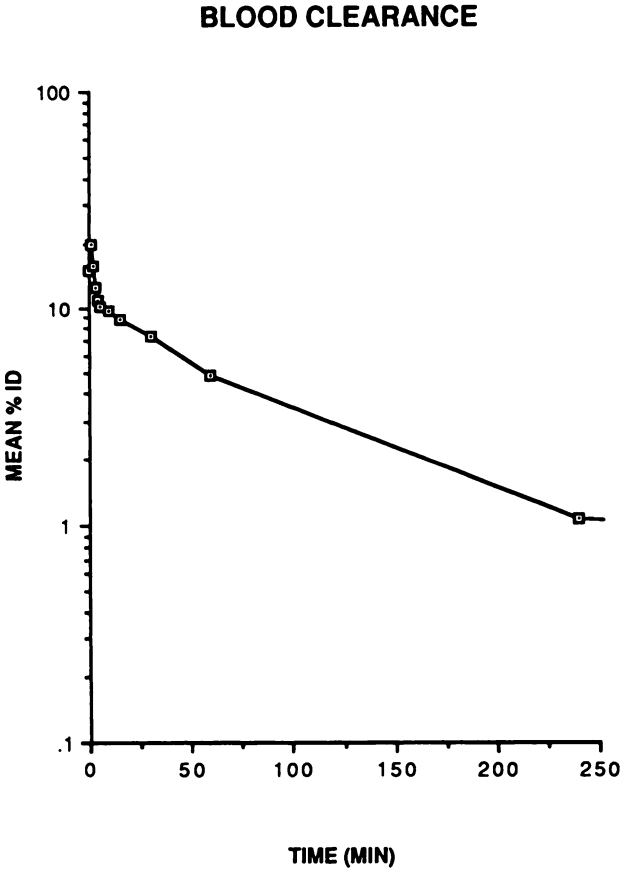

FIGURE 2
Mean blood clearance of [^{99m}Tc]ECD in normal subjects.

TABLE 1
Percent Injected Dose of [^{99m}Tc]ECD at Times After Injection

Organ	5 min	30 min	1 hr	2 hr	4 hr	24 hr
Brain	6.4 ± 2.1	5.7 ± 1.7	5.2 ± 1.3	4.7 ± 1.2	3.7 ± 0.3	2.1 ± 0.3
Lungs	4.6 ± 3.0	1.9 ± 1.9	1.4 ± 1.2	0.9 ± 0.8	0.6 ± 0.4	0.3 ± 0.2
Kidney	8.8 ± 2.9	4.0 ± 2.3	3.6 ± 1.8	1.8 ± 1.2	0.7 ± 0.4	0.4 ± 0.4
Bladder	8.3 ± 3.7	28.2 ± 10.3	21.8 ± 20.7	9.9 ± 17.0	2.9 ± 2.9	0.1 ± 0.1
Liver	15.0 ± 8.9	9.0 ± 6.2	5.4 ± 4.1	4.0 ± 2.6	2.2 ± 2.6	1.2 ± 0.6
Gallbladder	0.9 ± 1.1	2.6 ± 2.2	3.4 ± 2.7	4.2 ± 3.2	1.8 ± 1.5	0.2 ± 0.2

Percent injected dose/organ ± s.d.

ganglia, thalamus, and cerebellar hemispheres as regions of relatively increased tracer uptake in all normal subjects and on the side contralateral to the stroke in the 31 patients with unilateral stroke. In normal subjects, uptake was highest in the cerebellar hemispheres, occiptal cortex, and the basal ganglia followed by other regions of cortical gray matter (Fig. 3). White matter had substantially less uptake than gray matter.

The four regions in each hemisphere were labeled anterior (*1*), anterior central (*2*), posterior central (*3*), and posterior (*4*). On CT scan, stroke involved the anterior segment in five patients, the anterior central segment in 24, the posterior central segment in 21, and the posterior segment in eight patients.

Of the 34 patients with evidence of stroke on CT, 33 of the patients had focal [^{99m}Tc]ECD abnormalities on SPECT (97.1%) (Fig. 4). There was a discrepancy in the interpretation of one study, called normal by the blinded reviewer and abnormal by the nonblinded investigator, accounting for one false-negative study in this report. Of the 60 segments evidencing stroke on CT, 59 had decreased [^{99m}Tc]ECD on SPECT (98.3%). The one patient and the one segment with a normal [^{99m}Tc]ECD study was in a patient with evidence of a small infarct involving the basal ganglia on the CT scan.

Sixteen of the 34 patients with stroke had [^{99m}Tc] ECD perfusion defects extending into segments that were normal on CT (47.1%). In all 34 patients with stroke, 16 patients had [^{99m}Tc]ECD defects in the anterior segment, 26 in the anterior central segment, 27 in posterior central segment, and 11 in the posterior segment.

Crossed cerebellar diaschisis was present in 14 of 34 patients (41.2%) (Fig. 5). Ten of the 16 patients with defects extending into segments beyond those on CT (62.5%) and only four of 18 patients with [^{99m}Tc]ECD and CT scans that showed matching defects (22.2%) had decreased tracer uptake in the countralateral cerebellar hemisphere.

DISCUSSION

Technetium-99m ECD crosses the blood-brain barrier and is taken up rapidly by normal brain in a distribution proportional to regional cerebral blood flow (*13*). It is retained within the brain by rapid deesterification to a polar metabolite that does not recross the blood-brain barrier (*14*).

Our human biodistribution data confirm the observations made previously in animals. Brain uptake is rapid and peak brain activity compares favorably with other ^{123}I and ^{99m}Tc tracers, reaching over 6% of the injected dose by 5 min after intravenous injection. The pattern of [^{99m}Tc]ECD brain uptake in normal subjects was similar to that observed with [^{123}I]IMP with the highest activity in the cerebellar hemispheres, occipital lobe and the basal ganglia followed by other regions of the cerebal cortex (*15*). Other groups have reported similar brain distribution of the two tracers although lesions were better visualized with [^{99m}Tc]ECD SPECT because of the resulting higher contrast ratio and spatial resolution (*16*).

Blood clearance is rapid, resulting in high brain to soft-tissue activity ratios early after injection and improving with time for at least several hours after injection. Rapid lung clearance reduces further the problem of adjacent background activity during imaging. The rapid washout from facial muscles and from the salivary glands results in higher brain to soft-tissue ratios than have been reported for Tc-HM-PAO at comparable times after injection due to the more rapid blood clearance of [^{99m}Tc]ECD. As a result the optimal imaging time may be an hour or more after injection, after most of the soft-tissue activity has cleared.

The primary route of excretion of the tracer is through the kidneys. Consequently the critical organ is the urinary bladder. Assuming that the patient voids within 4.8 hr after injection and that the renal function is normal, an 18-mCi dose will result in a 5-rad exposure to the bladder wall and will also result in SPECT images of high technical quality. While this dose range is satisfactory for most routine studies, it may be necessary to inject some patients with two doses within a 24-hr period, especially if pharmacologic or physiologic intervention studies are contemplated. In this case, a substantially higher total dose (45 mCi) will give a 5-rad exposure to the bladder wall if the patient voids within 2 hr. Until biodistribution studies have been performed

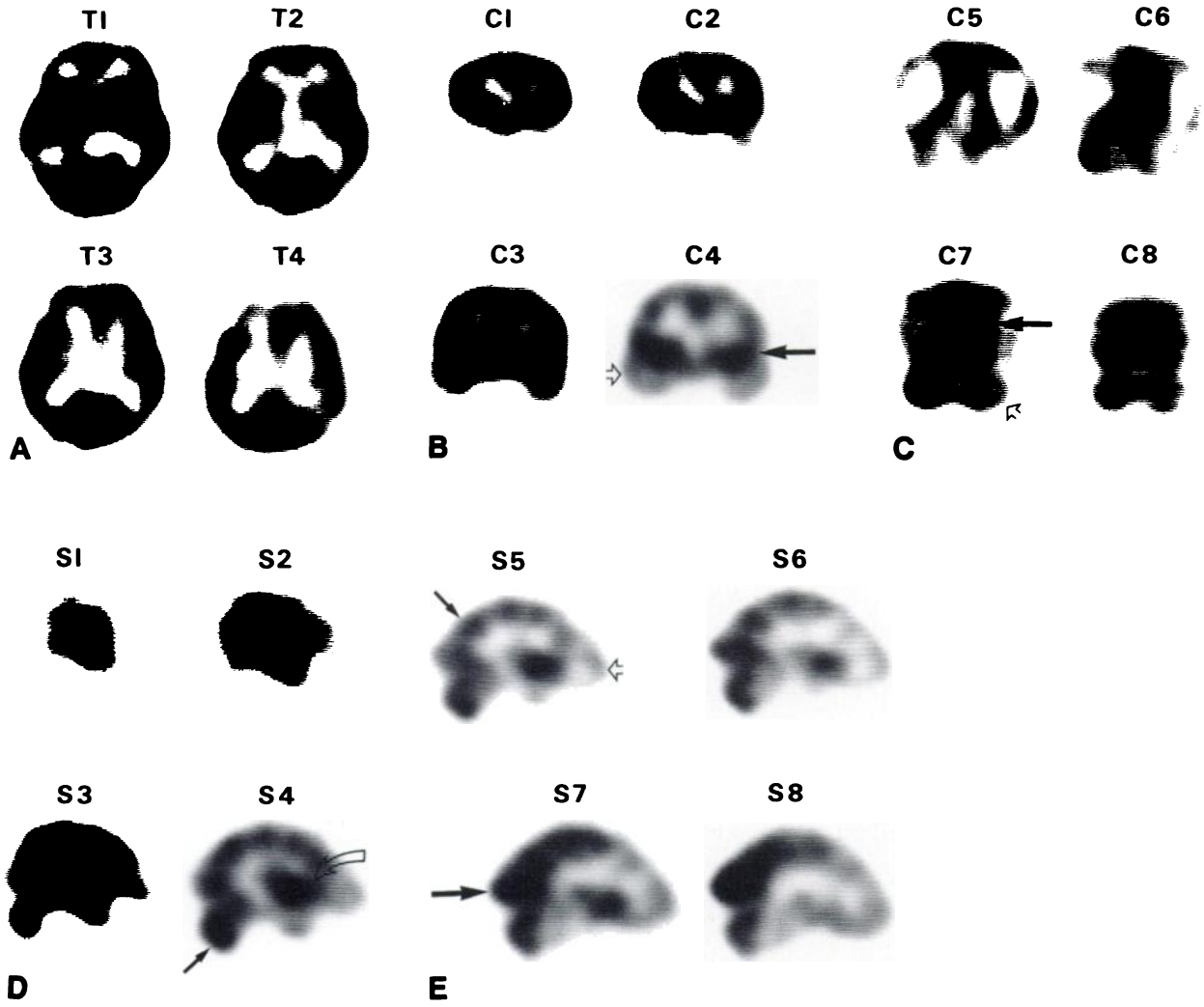

FIGURE 3
Technetium-99m ECD SPECT in normal subject. A: Transaxial slices obtained at the level of the basal ganglia and primary visual cortex (T1), 2 cm caudal to the basal ganglia (T2), and two slices obtained at the level of the interhemispheric fissure (T3, T4). B: Coronal slices obtained at the level of the anterior frontal lobe (C1, C2), and at the level of the basal ganglia (closed arrow) and temporal lobes (open arrow) (C3, C4). C: Coronal sections obtained posteriorly at the level of the parietal lobes (C5, C6) and at the level of the visual cortex (posterior occiptal lobe) (closed arrow) and cerebellar hemispheres (open arrow) (C7, C8). D: Sagittal images obtained at the level of the temporal lobe (S1, S2) and at the level of the basal ganglia (open arrow) and cerebellar hemisphere (closed arrow) (S3, S4). E: Medial sagittal planes at the level of the parietal lobe (closed arrow) and frontal pole (open arrow) (S5, S6) and adjacent to the interhemispheric fissure and through the occiptal lobe (primary visual cortex) (closed arrow) (S7, S8).

in patients with abnormal renal function, these patients should be studied using a more conservative dose regimen.

Our study suggests high brain clearance of the tracer during the first hour and a clearance averaging 10% per hour after that time. Our values are high because the measurements were obtained from planar data, resulting in an overestimation because of superimposed soft-tissue activity that has a very rapid initial clearance. Data based on SPECT studies (including a subset of our own normal subjects) indicate a slower clearance rate, averaging 12% per hour during the first hour and 5–6% per hour thereafter (*17*). Furthermore, there does not appear to be intracerebral redistribution of the tracer as is observed with [^{123}I]IMP. The [^{99m}Tc]ECD gray:white matter activity ratio remains high and constant over time when measured from sequential SPECT studies (*18*). If the tracer does not redistribute within the brain, the washout should not affect the quality of either the SPECT images or the data. Our images were uniformly high quality and the clearance did not affect the accuracy with which stroke was detected. Further, the SPECT data set could be corrected for clearance, if necessary.

Our data would suggest that [^{99m}Tc]ECD SPECT is an accurate method for the detection of stroke. Over 97% of patients and over 98% of strokes detected by x-ray CT had corresponding focal defects on the [^{99m}Tc]

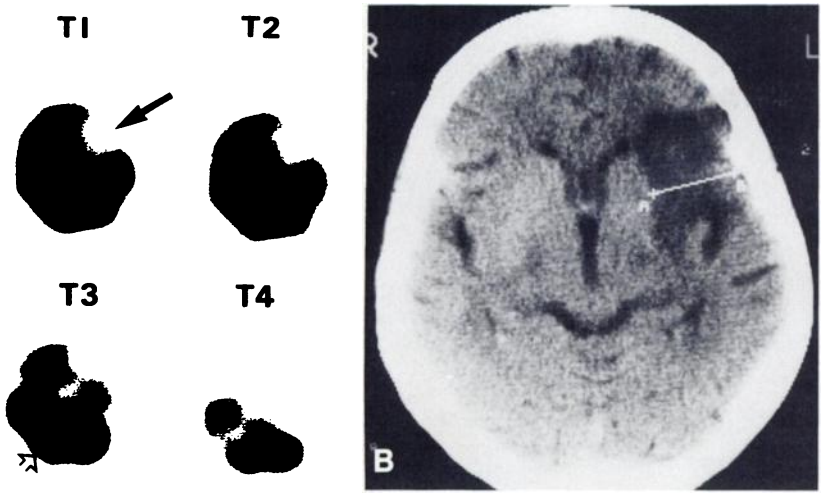

FIGURE 4
A: Technetium-99m ECD SPECT in a patient with left middle cerebral artery infarction. Note the focal defect (closed arrow) and crossed cerebellar diaschisis (open arrow). B: CT in the same patient. Note that the SPECT defect involves the same area as the abnormality on CT but also extends anterior to it.

ECD study. Our results are comparable to those obtained in patients with stroke following [^{123}I]IMP and [^{99m}Tc]HM-PAO SPECT (*4,19,20*). While our data was read by one observer blinded to clinical history and to the laboratory data, the entrance criteria may have resulted in a skewed population base. Each patient had an abnormal CT study prior to SPECT and the patient acquisition was not randomized. It is possible that the accuracy of the test would have been lower than we observed had the population been more representative.

As with [^{123}I]IMP SPECT, almost half of our patients had SPECT defects which were substantially larger than the extent of the infarct as measured from x-ray CT. The discordance between SPECT and CT might be due either to ischemic but viable tissue, to diffuse selective neuronal cell loss which may be present in zones surrounding an infarct, to decreased or absent metabolism along tracts made up of axons and dendrites of the infarcted neuron (Wallerian degeneration) (*21*), or to diaschisis, a decrease in the functional capacity and, hence, perfusion in a brain region caused by distant injury which occurs when excitatory impulses through afferent fiber tracts are interrupted, reducing the functional status of the distal region (*22*). Our observation that almost half of our patients have reduced [^{99m}Tc] ECD uptake in the contralateral cerebellar hemisphere in the absence of CT abnormalities indicates that the cerebellar assymetry, at least, is due to diaschisis and not due to cerebellar infarction or atrophy. Pantano et al. have observed a coupled decrease in blood flow and oxygen and glucose metabolism in these regions (*22*). Moretti et al. have observed a similar incidence of cerebellar diaschisis using [^{123}I]IMP SPECT (*23*). They observed no relation to diaschisis and clinical outcome although we found a higher incidence of cerebellar diaschisis when there was a substantial discordance in the extent of the cerebral abnormality between CT and SPECT.

As with other SPECT tracers of brain perfusion, [^{99m}Tc]ECD correlates with regional cerebral blood flow in normal tissue but the mechanisms for reduced uptake in stroke may be the result of a variety of causes including reduced blood flow, reduced tracer extraction, or reduced metabolism due to reduced oxygen and enzyme activity, leading to reduced tracer washout. To determine whether [^{99m}Tc]ECD is primarily a flow

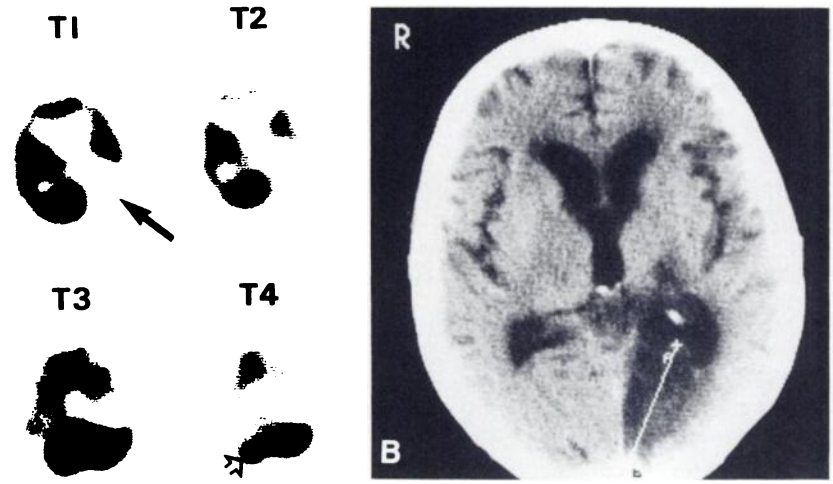

FIGURE 5
A: Technetium-99m ECD SPECT in a patient with posterior cerebral infarction. There is a focal defect involving the posterior temporal and parietal lobes in the distribution of the posterior cerebral artery (closed arrow). Note crossed cerebellar diaschisis (open arrow). B: CT in the same patient with evidence of a large posterior cerebral artery infarction.

tracer or may be affected by metabolism, studies will have to be carried out in patients with subacute stroke and with uncoupling of metabolism and blood flow (luxury perfusion).

In summary, [^{99m}Tc]ECD is a promising tracer for the evaluation of patients with stroke. High quality SPECT imaging results from the optimal physical characteristics of ^{99m}Tc and the favorable biodistribution of ECD which results in low background activity, high photon flux, and high brain uptake.

ACKNOWLEDGMENT

The authors thank Michael Stabin, Oak Ridge Associated Universities, for providing the dosimetry estimates. We also acknowledge the assistance of our co-investigators: M. Picard, MD, Hopital Saint Luc, Montreal; R. Tikofsky, PhD, Medical College of Wisconsin; B. D. Collier, MD, Medical College of Wisconsin; S. Vallabhajosula, PhD, Mt. Sinai Medical Center; J. Meyer, MD, Harbor-UCLA Medical Center; J. Kuperus, MS, Harbor-UCLA Medical Center; A. Gagnon, CNMT, Hotel Dieu de Montreal; G. Taddie, MD, S. Rafaele; M. Zito, PhD, S. Rafaele; N. Vigneron, MD, Henri Mondor; B. Delaloge, MD, Centre Hospitalier, Universitaire Vaudois; G. Robbins, MD, New England Deaconess Hospital; D. C. Costa, MD, University College and Middlesex School of Medicine; and L. Verhaegen, CNMT, V. Z. Gasthuisberg.

REFERENCES

1. Winchell HS, Horst WA, Braum L, Oldendorf WH, Hattern R, Parker H. N-isopropyl (I123) p-iodoamphetamine: single-pass brain uptake and washout: binding to brain synaptosomes: and localization in dog and monkey brain. *J Nucl Med* 1980; 21:947–952.
2. Hill TC, Holman BL, Lovett R, et al. Initial experience with SPECT (single-photon computerized tomography) of the brain using N-isopropyl I-123 p-iodoamphetamine. *J Nucl Med* 1982; 23:1911–1995.
3. Holman BL, Lee RGL, Hill TC, et al. A comparison of two cerebral perfusion tracers N-isopropyl I-123 p-iodoamphetamine and I-123 HIPDM in the human. *J Nucl Med* 1984; 25:25–30.
4. Hill TC, Magistretti PL, Holman BL, et al. Assessment of regional cerebral blood flow (rCBF) in stroke using SPECT and N-isopropyl-(I-123)-p-iodoamphetamine (IMP). *Stroke* 1984; 15:40–45.
5. Defer G, Moretti J-L, Cesaro P, Sergent A, Raynaud C, Degos J-D. Early and delayed SPECT using N-isopropyl p-iodoamphetamine iodine 123 in cerebral ischemia: a prognostic index for clinical recovery. *Arch Neurol* 1987; 44:715–718.
6. Johnson KA, Mueller ST, Walshe TM, English RJ, Holman BL. Cerebral perfusion imaging in Alzheimer's disease. *Arch Neurol* 1987; 44:165–168.
7. Magistretti P, Uren P, Schomer D, Blume H, Holman BL, Hill TC. Emission tomographic scans of cerebral blood flow using I-123 iodoamphetamine in epilepsy. In: Raynaud C, ed. *Proceedings of the Third World Congress of Nuclear Medicine and Biology.* Oxford: Pergamon Press, 1982: 139–143.
8. Volkert WA, Hoffman TJ, Seger RM. Tc-99m propyleneamine oxime (Tc-99m-PnAO): a potential brain radiopharmaceutical. *Eur J Nucl Med* 1984; 9:511–516.
9. Sharp PF, Smith FW, Gemmell HG, et al. Technetium-99m-HM-PAO stereoisomers as potential agents for imaging regional cerebral blood flow. *J Nucl Med* 1986; 27:171–177.
10. Lever SZ, Burns HD, Kervitsky TM, et al. The design, preparation and biodistribution of a technetium-99m triaminodithiol complex to assess regional cerebral blood flow. *J Nucl Med* 1985; 26:1287–1294.
11. Kung HF, Molnar M, Billings J. Synthesis and biodistribution of neutral lipid-soluble Tc-99m complexes that cross the blood-brain barrier. *J Nucl Med* 1984; 25:326–332.
12. Cheesman EH, Blanchette MA, Ganey MV, Maheu LJ, Miller SJ, Watson AD. Technetium-99m ECD: ester-derivatized diamine-dithiol Tc complexes for imaging brain perfusion [Abstract]. *J Nucl Med* 1988; 29:788.
13. Walovitch RC, Williams SJ, Morgan RA, Garrity ST, Cheesman EH. Pharmacology characterization of Tc-99m ECD in non-human primates as a new agent for brain perfusion imaging [Abstract]. *J Nucl Med* 1988; 29:788.
14. Walovitch RC, Hall KM, O'Toole JJ, Williams SJ. Metabolism of Tc-99m-ECD in normal volunteers [Abstract]. *J Nucl Med* 1988; 29:747.
15. Johnson KA, Holman BL, Mueller SP, et al. Single photon emission computed tomography in Alzheimer's disease: abnormal iofetamine I-123 uptake reflects dementia severity. *Arch Neurol* 1988; 45:392.
16. Moretti JL, Defer G, Cinotti L, Cesaro P, Vigneron N, Pethe C. Comparative tomoscintigraphic study of strokes using ECD Tc-99m, HMPAO Tc-99m and IMP I-123. *Eur J Nucl Med* 1988; 12:311.
17. Franceschi M, Picard M, Zimmerman RE, Kronauge JF, Jones AG, Holman BL. Brain washout of Tc-99m-L, L-ethyl cysteinate dimer (ECD) in normal volunteers. *Eur J Nucl Med* 1988; 14:227.
18. Leveille J, Demonceau G, Rigo P, De Roo M, Taillefer R, Burgess BA, Morgan RA, Wallovitch RC. Brain tomographic imaging with Tc-99m-ethyl cysteinate dimer (Tc-ECD): a new stable brain perfusion agent [Abstract]. *J Nucl Med* 1988; 29:758.
19. Ell PJ, Hocknell JML, Jarrit PH. Tc-99m-labelled radiotracer for the investigation of cerebrovascular disease. *Nucl Med Commun* 1985; 6:437–441.
20. Berberich A, Buell U, Eilles A, Gerhards W, Jaeger A, Ferbert A, Moser E. (HMPAO) SPECT in cerebrovascular disease: a comparison to transmission CT [Abstract]. *J Nucl Med* 1986; 27:888.
21. Jolesz FA, Polak JF, Ruenzel PW, Adams DF. Wallerian degeneration demonstrated by magnetic resonance: spectroscopic measurements on peripheral nerve. *Radiology* 1984; 152:85–87.
22. Pantano P, Baron JC, Samson Y, Bousser MG, Derouesne C, Comar D. Crossed cerebellar diaschisis. *Brain* 1986; 109:677–694.
23. Moretti JL, Cesaro P, Louarn F, et al. N isopropyl amphetamine I-123 et tomoscintigraphie monophotonique dans les affections ischemiques cerebrales. *Cir et metab due cerveau* 1984; 2:63–75.